Antarctic Clouds and Radiation within the NCAR Climate Models*

KEITH M. HINES AND DAVID H. BROMWICH

Polar Meteorology Group, Byrd Polar Research Center, The Ohio State University, Columbus, Ohio

PHILIP J. RASCH

National Center for Atmospheric Research, Boulder, Colorado

MICHAEL J. IACONO

Atmospheric and Environmental Research, Inc., Lexington, Massachusetts

(Manuscript received 28 February 2003, in final form 9 September 2003)

ABSTRACT

To evaluate and improve the treatment of clouds and radiation by the climate models of the National Center for Atmospheric Research (NCAR), simulations by the NCAR Community Climate Model version 3 (CCM3), as well as the recently released Community Atmosphere Model version 2 (CAM2), are examined. The Rasch and Kristjánsson prognostic cloud condensate scheme, which is now the standard scheme for CAM2, is included in a version of CCM3 and evaluated. Furthermore, the Rapid Radiative Transfer Model (RRTM), which alleviates the deficit in downward clear-sky longwave radiation, is also included in a version of CCM3. The new radiation scheme in CAM2 also alleviates the clear-sky longwave bias, although RRTM is not included. The impact of the changes is especially large over the interior of Antarctica. The changes induced by the introduction of the prognostic cloud scheme are found to have a much larger impact on the CCM3 simulations than do those from the introduction of RRTM. The introduction of the prognostic cloud scheme increases cloud emissivity in the upper troposphere, reduces cloud emissivity in the lower troposphere, and results in a better vertical distribution of cloud radiative properties over interior Antarctica. The climate simulations have a very large cold bias in the stratosphere, especially during summer. There are significant deficiencies in the simulation of Antarctic cloud radiative effects. The optical thickness of Antarctic clouds appears to be excessive. This contributes to a warm bias in surface temperature during winter and a deficit in downward shortwave radiation during summer. Some biases for Antarctica are larger for CCM3 with the prognostic cloud condensate scheme than with the standard diagnostic clouds. When the mixing ratio threshold for autoconversion from suspended ice cloud to falling precipitation is reduced toward a more realistic value, the Antarctic clouds are thinned and some of the biases are reduced. To improve the surface energy balance, not only must the radiative effects of clouds be improved, it is also necessary to improve the representation of sensible heat flux. Insufficient vertical resolution of the frequently very shallow, very stable surface boundary layer apparently contributes to an excessive heat flux from the atmosphere to the surface during winter. The representations of Antarctic clouds and radiation by the new NCAR CAM2 are not clearly improved compared to those of the earlier CCM3. For example, the surface albedo over Antarctica is descreased in CAM2 and Community Climate System Model version 2 (CCSM2) simulations in comparison to CCM3 simulations, contributing to a summer warm bias in tropospheric temperature for the former.

1. Introduction

The largest variance between the results of global climate models is found in the polar regions (e.g., Gates et al. 1996). This is not surprising given that the polar regions present unique challenges. Cloud radiative effects, in particular, require special attention, because modeling efforts must account for such phenomena as clear-sky precipitation and Arctic haze, while also dealing with extremely low surface temperatures and atmospheric moisture contents. Cloud emissivities are frequently much less than 1 (Lubin and Harper 1996; Randall et al. 1998). The radiative flux is concentrated in different parts of the infrared spectrum than in warmer, wetter climates (Curry et al. 1996; Randall et al. 1998). Furthermore, the near-surface air is often saturated or supersaturated with respect to ice (Anderson 1993). Many common modeling parameterizations are designed for other environments and may not work well

* Byrd Polar Research Center Contribution Number 1285.

Corresponding author address: Keith M. Hines, Polar Meteorology Group, Byrd Polar Research Center, The Ohio State University, 1090 Carmack Road, Columbus, OH 43210.
E-mail: hines.91@osu.edu

in polar regions (Pinto and Curry 1997; Randall et al. 1998). Fortunately, recent sizeable efforts, such as the Surface Heat Budget of the Arctic Ocean (SHEBA; Randall et al. 1998) and the First International Satellite Cloud Climatology Project (ISCCP) Regional Experiment (FIRE; Curry et al. 2000), are generating knowledge about clouds and radiative processes and their interactions in the Arctic. As a result of this work, adjustments to the parameterizations of clouds and radiation have been shown to significantly improve column model and mesoscale simulations in the Arctic (e.g., Pinto et al. 1999; Girard and Curry 2001).

The Antarctic region also requires special attention. While water clouds are often present in the Arctic, the clouds over continental Antarctica consist primarily of ice crystals (Morely et al. 1989). Furthermore, the concentration of condensation nuclei can be extremely low (A. Hogan 2001, personal communication). Modeling studies show that the simulated high southern latitude climate is highly sensitive to the radiation parameterization (e.g., Shibata and Chiba 1990; Lubin et al. 1998).

Simulations with previous generations of the National Center for Atmospheric Research (NCAR) climate models have demonstrated the difficulties representing the hydrologic cycle and radiative effects for the polar regions in general, and for Antarctica in particular. The inclusion of the semi-Lagrangian advection scheme and the increased horizontal resolution to T42 (about 2.8° latitude $\times$ 2.8° longitude) in the Community Climate Model version 2 (CCM2), removed the excess polar precipitation simulated by its predecessor CCM1 with R15 resolution (Tzeng et al. 1993, 1994). Other improvements simulated with CCM2 included a much improved location and intensity of the circumpolar trough, the intensity and horizontal distribution of the surface inversion, and the arid climate over Antarctica. Nevertheless, CCM2 included deficiencies such as significantly overestimated summertime cloud cover, contributing to a cold bias and shortwave deficit over Antarctica (Tzeng et al. 1994).

During the latter half of the 1990s, CCM3 became the state-of-the-art atmospheric climate model at NCAR. Briegleb and Bromwich (1998a,b) examine the polar climate and radiation balance simulated by this enhanced model. They find that CCM3 simulates a much improved pattern of sea level pressure near Antarctica compared to that of CCM2. Overall, the polar climate of CCM3 is an incremental improvement over that simulated by CCM2. Biases, however, still remain in the simulated polar radiation budget despite overall improvements in the global radiation (Kiehl et al. 1998b; Briegleb and Bromwich 1998b). There is a summer deficit of absorbed shortwave radiation of about 20 W m^{-2} for both polar regions, because the polar clouds are apparently too reflective. Furthermore, there is a deficit of at least 10 W m^{-2} in the downward clear-sky longwave radiation during the South Pole winter. Briegleb and Bromwich (1998a,b) suggest that the causes of remaining deficiencies in the NCAR CCM3 include the following: 1) inadequate cloud cover and optical property representation, 2) inadequate surface albedo over sea ice and the Antarctic plateau, 3) systematic deficit in surface downward longwave radiation, 4) inadequate representation of the sea ice–atmosphere heat exchange, resulting from the lack of both fractional sea ice coverage and variability of sea ice thickness, 5) limitations due to the T42 horizontal resolution, and 6) biases in the influence from the Tropics and midlatitudes. A recent emphasis of the NCAR climate modeling community is in improving the treatment of clouds and cloud radiative effects. Therefore, we will consider points 1–3 in this paper. Points 4–6 also need to be explored, although they are outside the context of this study on Antarctic clouds and radiation.

While Briegleb and Bromwich (1998b) report on the status of CCM3's polar radiation simulation, in this paper we expand the evaluation to include new parameterizations and recent public versions of the NCAR climate models. As a complement to the considerable recent focus on climate modeling in the Arctic, we choose to concentrate here on the Antarctic region. We examine how the simulated climate responds to changes in polar cloud and radiation parameterizations, and how the simulated climate can be improved.

2. NCAR climate models

Several configurations of the cloud and radiation parameterizations for the NCAR CCM3 are evaluated. Additionally, atmospheric output is evaluated for two benchmark simulations with standard versions of the new NCAR atmospheric model Community Atmosphere Model version 2 (CAM2), and the new NCAR coupled Community Climate System Model version 2 (CCSM2). The model CCM3, with T42 resolution and 18 levels in the vertical, has refinements in the cloud parameterization over that of the earlier CCM2 (Kiehl et al. 1998a). The diagnostic parameterizations for cloud fraction in standard CCM3, nearly identical to those of CCM2, are based upon improvements to the model of Slingo (1987). Cloud fraction is determined from the relative humidity, with vertical velocity, static stability, and convective mass flux as additional inputs. Clouds can exist at all tropospheric levels above the surface layer. Optical properties of liquid water droplets are also parameterized the same way in both CCM2 and CCM3, based on the model of Slingo (1989). Major refinements to CCM3 involve the allowance for ice clouds as well as water clouds, and the difference in cloud particle sizes over land versus water. Over the ocean, cloud liquid water droplet effective radius is fixed at 10 μm, as was done globally in the original version of CCM2 (Hack et al. 1993). Over land, cloud liquid water droplet effective radius is fixed at 5 μm in air warmer than -10°C, with a linear increase in droplet effective radius with temperatures between -10° and -30°C. Between -10°

TABLE 1. CCM3 and CAM2 simulations.

Simulation	Model	Cloud scheme	Longwave radiation scheme	Sea surface temperature
Climate SST	CCM3	CCM3 standard	CCM3 standard	Climatological SST
AMIP SST	CCM3	CCM3 standard	CCM3 standard	AMIP
Predicted Cloud Water	CCM3	Predicted cloud condensate	CCM3 standard	AMIP
RRTM	CCM3	CCM3 standard	RRTM	AMIP
PCW + RRTM	CCM3	Predicted cloud condensate	RRTM	Climatological SST
Thin Cloud	CCM3	Predicted cloud condensate	RRTM	Climatological SST
Thick Cloud	CCM3	Predicted cloud condensate	RRTM	Climatological SST
CAM2	CAM2	Predicted cloud condensate	CAM2	Climatological SST

and −30°C, the fraction of total cloud water that is ice is specified to increase linearly from 0 to 1. Ice particle effective radius is specified as a function of atmospheric pressure, varying from 10 μm in the lower troposphere (pressures greater than 0.7 of surface pressure) to a maximum of 30 μm in the upper troposphere (pressures less than 0.4 of surface pressure). Optical properties of ice particles are taken from Ebert and Curry (1992). The radiative effects of nonspherical cloud particles are not accounted for, although Kristjánsson et al. (1999) find that the shape of ice cloud particles may have a large impact on the radiative properties. The vertical distribution of cloud condensate is prescribed based upon the vertically integrated water vapor.

The model also incorporates the NCAR Land Surface Model (LSM; Bonan 1996). In calculating the albedo over snow-covered land, the LSM considers two radiative bands, visible and near-infrared (Bonan 1996). Based upon the work of Marshall (1989), modeled snow albedo decreases as the solar elevation angle increases, the soot content increases, and the snow grain radius increases. The typical CCM3 snow grain radius is 100 μm for Antarctica.

The NCAR CCSM2 includes CAM2 for the atmospheric component, along with prognostic sea ice, land, and ocean components. The results of the CAM2 and CCSM2 simulations will differ because the benchmark CAM2 simulation has prescribed climatological surface boundary conditions, while the CCSM2 simulation has simulated surface conditions that include interannual variability. The CAM2 has a standard horizontal resolution of T42 and 26 levels in the vertical (Collins et al. 2003). The difference in vertical resolution between CCM3 and CAM2 is primarily concentrated near the tropopause. The revised NCAR climate models have a new Community Land Model, version 2.0, and many other new features. Furthermore, the atmospheric model CAM2 now includes the Collins (2001) scheme to allow for a greater variety of cloud overlap assumptions, new water vapor absorptivity and emissivity (Collins et al. 2002), improved representations of ozone and topography, and evaporation of precipitation.

The CCM3 simulations include two standard benchmark simulations performed by NCAR: a 14-yr simulation, which includes the period of the Atmospheric Model Intercomparison Project (AMIP) beginning in 1979, which we will refer to as AMIP SST; and 10 yr of a simulation with climatological boundary conditions recycled every year, which we shall refer to as Climate SST. In addition to the benchmark simulations with a standard version of CCM3, we also consider a CCM3 simulation, which we shall refer to as Predicted Cloud Water (PCW), with the standard global scheme for diagnostic cloud water and ice replaced with the more sophisticated predictive scheme of Rasch and Kristjánsson (1998). With this scheme, clouds consist of ice particles (liquid drops) for temperatures below −20°C (above 0°C), and are mixed phase for temperatures between −20° and 0°C. The scheme is simple enough to be computationally efficient. Nevertheless, the scheme can treat a much broader variability of cloud condensate than was allowed by the previous scheme, which prescribed the vertical distribution of condensate as function of the column-integrated water vapor. The prognostic scheme was anticipated to provide a more realistic depiction of Antarctic clouds. Rasch and Kristjánsson (1998) found that the largest sensitivity to the change in cloud scheme is located in the Arctic during winter and in the Antarctic for all seasons. The simulated seasonal cycle of cloud amount in the Arctic was improved by the change. The simulation of Predicted Cloud Water is for 14 yr over the same time period as AMIP SST. These simulations are listed in Table 1.

Also, Atmospheric and Environmental Research, Inc., has provided a version of the Rapid Radiative Transfer Model (RRTM; Mlawer et al. 1997; Iacono et al. 2000), a longwave radiation code that can be included in CCM3. For clear skies, this radiation code yields larger downwelling longwave fluxes for polar atmospheric conditions than the standard version of the CCM3 radiation code. Radiation calculations for a column model with RRTM by Walden show that it produces close agreement with line-by-line radiation calculations, thus, eliminating the polar clear-sky longwave bias found in many atmospheric climate models (see the Web page online at http://polarmet.mps.ohio-state.edu/walden/rrtm_verify.html). Pinto et al. (1999) also used RRTM to improve Arctic longwave radiation in column model simulations. Therefore, we include in the model comparison a 10-yr simulation referred to as RRTM that was performed by Atmospheric and Environmental Research, Inc., for the AMIP period.

To seek improved climate simulations, both the prognostic cloud particulate scheme of Rasch and Kristjánsson (1998) and RRTM (Iacono et al. 2000) are implemented in CCM3, version 3.6. A 15-yr simulation with climatological boundary conditions is performed. We refer to this new simulation as PCW + RRTM. Results are compared to the other CCM3 simulations.

In our comparison, we include simulations performed at different times and locations by different persons. Therefore, some minor differences in the versions of CCM3 employed will occur. These differences are generally minor and the effect appears to be small, much less than those arising from the changes in the parameterizations of clouds and radiation. Some of the simulations have annually varying boundary conditions for fields such as sea surface temperature. It was found, however, that the multiyear average fields for clouds and radiation are very similar for the simulations of Climate SST and AMIP SST. Therefore, the differing boundary conditions do not appear to have a first-order effect on the simulations. For simplicity, only the results of Climate SST are shown in the analysis that follows. The CCM3 simulation RRTM does show some differences from the other simulations resulting from other causes besides the longwave radiation scheme. For instance, there are increased stratospheric clouds in RRTM. Nevertheless, we believe that the differences between simulations are large enough that the first-order effects can be safely attributed to intended changes in the cloud and radiation schemes.

3. High southern latitude temperature

The CCM3 results show a high sensitivity to the clouds and radiation parameterizations over Antarctica. Figure 1 shows the monthly surface temperature at the South Pole and the winter (June, July, and August) and summer (December, January, and February) values as a function of latitude for several simulations. The results for the CAM2 simulation will be discussed in section 4. North of the pack ice surrounding Antarctica, CCM3 ocean surface temperature is specified and is not sensitive to the changes in parameterization (Figs. 1a and 1b). The latitudes of largest winter sensitivity are south of 75°S, indicating that the greatest sensitivity is over interior Antarctica. Therefore, we will focus on the interior of Antarctica. The observations in Fig. 1c show the 1957–2002 monthly average surface air observations at Amundsen-Scott Station (90°S) from the Reference Antarctic Data for Environmental Research (READER) dataset compiled by the Scientific Committee on Antarctic Research and available through the British Antarctic Survey's Web site (online at http://www.antarctica.ac.uk/met/READER/). Estimated surface temperature for 1982–99 from the extended Advanced Very High Resolution Radiometer (AVHRR) Polar Pathfinder dataset (Key 2001) is also shown. The AVHRR temperature is an average of temperatures at

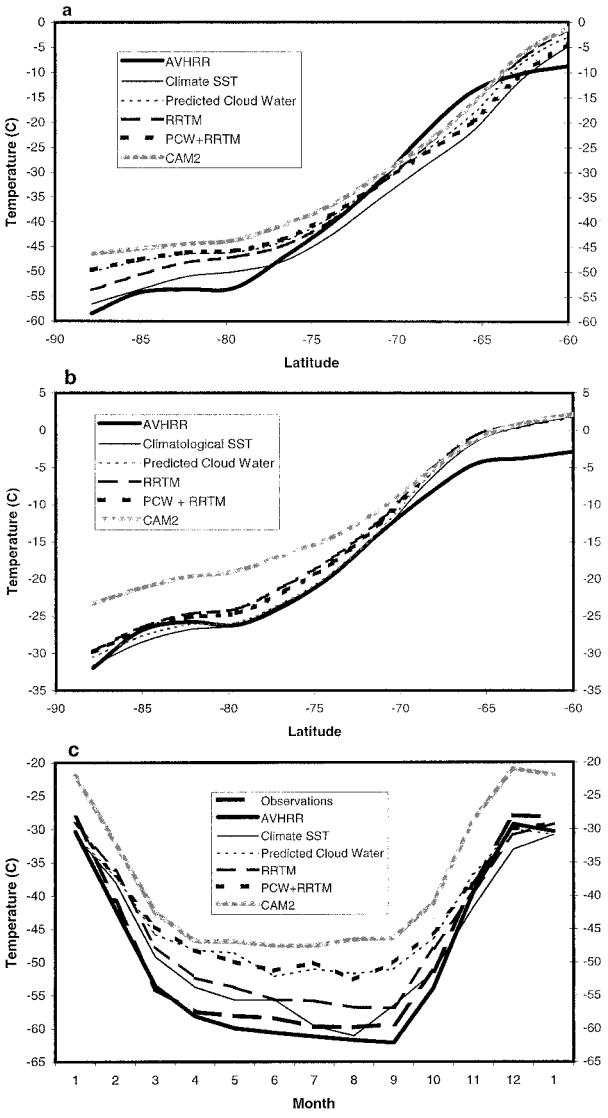

FIG. 1. Surface temperature (°C) from observations, satellite retrievals, and CCM3 and CAM2 model runs. Mean 3-month values versus latitude are shown for (a) winter (Jun–Jul–Aug) and (b) summer (Dec–Jan–Feb), and (c) monthly values at the South Pole vs time are displayed.

1400 and 0200 local solar times. Figure 1c shows that the AVHRR-derived surface temperature provides a reasonable estimate of the observed value. The AVHRR values are about 2°C colder than the observed temperature during winter, perhaps due to the temperature difference between the near-surface air and the typically colder snow surface. The surface temperature for simulations with the standard version of CCM3, Climate SST, and AMIP SST are very similar; hence, only the results for Climate SST are shown.

The differences seen in Fig. 1c are generally too large to be attributed to model topography. Model surface height interpolated to the South Pole is 2972 m for CCM3 and 2775 m for CAM2, while the Clean Air

Automatic Weather Station is located at 2835 m. The surface temperature change with height along the surface of interior Antarctica tends to follow the dry adiabatic lapse rate. To adjust for the height difference, we add 1.34°C to the CCM3 values and subtract 0.59°C to the CAM2 values in Fig. 1c. The difference between observed and simulated temperature is usually larger than 2°C, so other factors besides topography must be important.

Except for September, the standard version of CCM3 shows a reasonable surface temperature for late winter and spring. The early onset of cold winter temperature, beginning about April, however, is not well captured by CCM3. During the brief summer at the South Pole, when shortwave radiation is an important component of the surface energy balance, the standard version of CCM3 is up to 5°C too cold. The simulation with the RRTM radiation code is about 5°C warmer than observations during winter and slightly colder than the observations during summer. These warmer surface temperatures in RRTM than in Climate SST are consistent with an increase in downward clear-sky radiation. Figure 1c indicates that the inclusion of prognostic cloud water in the simulations of Predicted Cloud Water, and PCW + RRTM has a much larger impact than the inclusion of the RRTM code. The warmest CCM3 simulations are Predicted Cloud Water and PCW + RRTM. The surface temperatures for these simulations are as much as 10°C too warm during winter. Summer surface temperatures are less sensitive to the CCM3 parameterizations.

Figure 2 shows the 3-month average vertical temperature profiles for winter (June–July–August) and summer (December–January–February) at the South Pole. The observed profile for summer is from a composite of the 1961–2000 climatological values at standard levels (500, 300, 200, 150, 100, and 50 hPa), the 1957–2002 values at the surface, and 1988–90 rawinsonde measurements from the READER dataset (Fig. 2b). The rawinsondes provide a representation of the temperature profile in the lower troposphere. For winter, the temperature profile within the strong inversion is not be well represented by the rawinsondes (e.g., Mahesh et al. 1997). Therefore, the surface and standard level temperature data for Fig. 2a are supplemented by Schwerdtfeger's (1984) temperature profile for the winter boundary layer. There are some differences in surface pressure for Fig. 2 due to representations of topography by the NCAR models. The largest differences in temperature between the different model configurations are located in the lower troposphere. The standard version of CCM3 produces the coldest profiles in the lower troposphere. The RRTM simulation shows a slight warming, mostly in the lowest 50 hPa of the troposphere. Predicted Cloud Water shows a much larger warming in the lower troposphere. The top of the inversion for this simulation is about 4°C warmer during summer and 2°C warmer during winter compared to that of standard CCM3. The simulation PCW + RRTM is slightly colder at most levels than that of Predicted Cloud Water, but the difference is almost always less than 2°C.

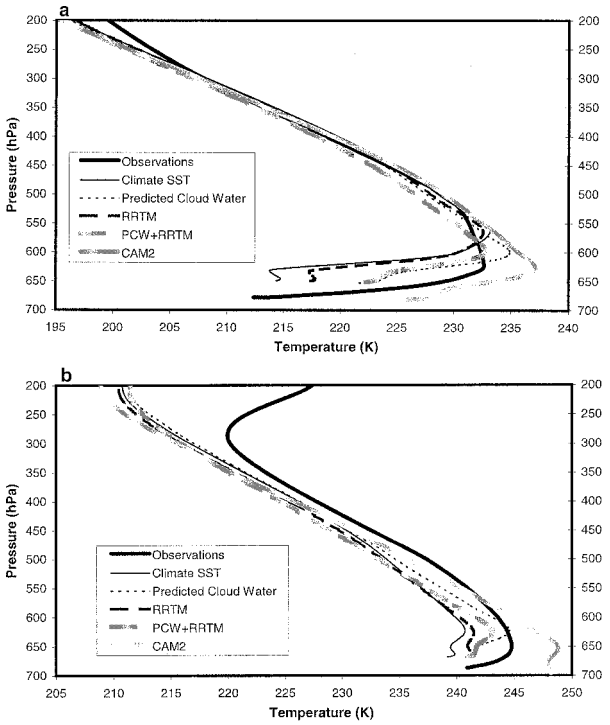

FIG. 2. Vertical profiles of 3-month average temperature (K) from observations and model results at the South Pole for (a) winter and (b) summer. Observations are compiled from multiyear observations at standard pressure levels and the surface from the READER dataset. Summer profiles are supplemented by 1988–90 rawinsonde observations, and the winter profile is supplemented by the Schwerdtfeger (1984) boundary layer profile.

The intensity of the winter inversion is well captured by Climate SST, the simulation with the standard version of CCM3. The depth of the inversion, however, is about 85 hPa rather than about 50 hPa for the observations. Other configurations of the NCAR climate models underrepresent the inversion intensity. For example, the simulation PCW + RRTM has an inversion intensity about 9°C smaller than that of the observations. Furthermore, there are weak minima in the temperature profiles for Climate SST and RRTM about 20 hPa above surface. The use of the prognostic cloud condensate scheme eliminates these spurious minima, and the inversion depths for the simulations Predicted Cloud Water and PCW + RRTM are close to the observed depth. For these simulations, the modified temperature lapse rate in the lowest model levels has consequences for the sensible heat flux. This will be discussed in section 7. The prognostic cloud condensate scheme, in addition to having more impact than the RRTM longwave radiation, results in some qualitative improvements for the Antarctic temperature profile. Nevertheless, all of the simulations exaggerate the sharpness of the lower-tropospheric temperature profile near the temperature maxi-

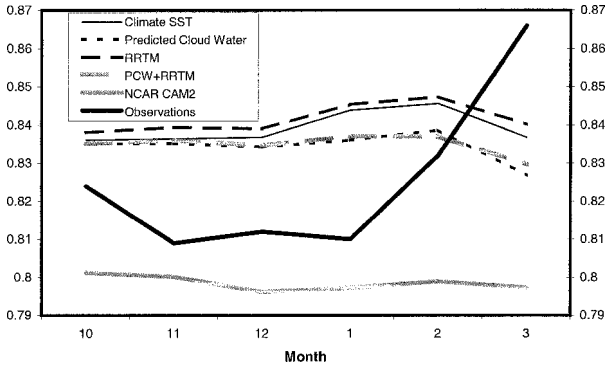

FIG. 3. Monthly surface albedo at the South Pole.

mum. The observations for winter, on the other hand, show a layer with a weak lapse rate between 525 and 630 hPa. There is a significant cold bias during summer at most levels for the CCM3 simulations. This bias is exceptionally large in the stratosphere where it can reach 20°C. Cold biases at the tropopause are a pervasive problem for global climate models for reasons that are not clear. In the following sections, we shall attempt to explain and interpret the results seen in Figs. 1 and 2.

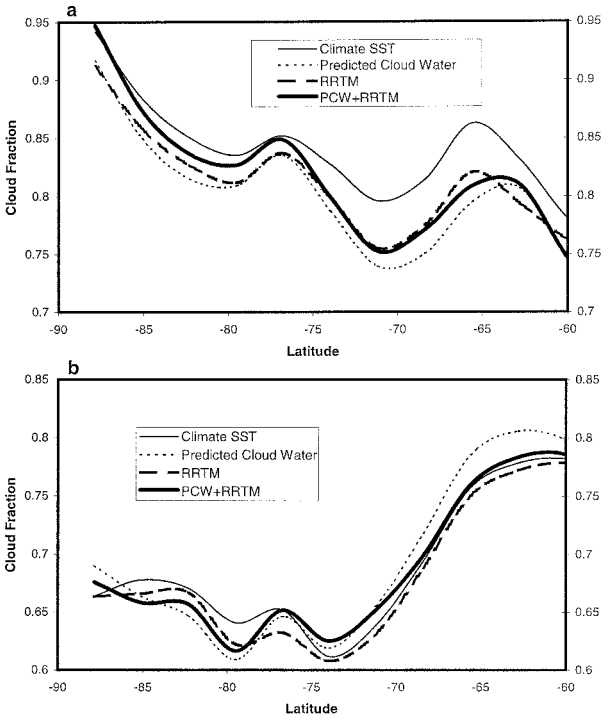

FIG. 4. Three-month average total cloud fraction vs latitude for (a) winter and (b) summer.

4. Surface albedo

The summer temperature field is highly influenced by the surface albedo. Figure 3 shows the monthly surface albedo at the South Pole from October to March. Observed values are obtained from climatological radiation measurements provided by J. King (1997, personal communication). The observed albedo over interior Antarctica does not display a large seasonal cycle unlike the Arctic case in which summer melting significantly reduces the surface reflection (e.g., Briegleb and Bromwich 1998b). South Pole values for CCM3 vary from 0.83 to 0.85 and are obtained from the LSM linked with the atmospheric model. Observations suggest an albedo of about 0.81 during the summer. The value is slighter larger during spring and autumn when the sun is close to the horizon. The surface radiation balance can be highly sensitive to the albedo over an ice surface because a change in albedo from just 0.80 to 0.81 results in a 5% reduction in absorbed shortwave radiation. Therefore, some of the summer cold bias in Figs. 1 and 2 for summer may result from a slightly large albedo. For CAM2, by contrast, the albedo is somewhat smaller, in the range 0.79–0.80. The reduction in Antarctic summer albedo with the introduction of the new Community Land Model for CCSM2 appears to be an important difference from the earlier LSM. The resulting increase in absorbed shortwave radiation contributes to the large warm bias in the lower troposphere during summer for the most recent generation of NCAR climate models (Figs. 1 and 2). In summary, Figs. 1–3 suggest that the best estimate of surface temperature for the Antarctic summer may be achieved with an albedo between that of CCM3 and CAM2.

5. Cloud fraction

The observed cloud fraction over the South Pole is about 35% during winter and 55% during summer (Hahn et al. 1995). In contrast, the observed cloud fraction is about 75% along the Antarctic coast, because the cloud cover is large near the strong minimum in sea level pressure along the Antarctic circumpolar trough. Mahesh et al. (2001a) find that South Pole clouds have a seasonally dependent bimodal distribution in height, with a cloud base frequently found in the upper boundary layer, and a second maximum frequency located near 2.0–2.5 km above the surface. They find that cloud-base height is more variable during summer. The cloud fraction for the models CCM3 and CAM2 is based upon a diagnostic Slingo-type scheme. For the standard version of CCM3, this scheme is more heavily used within the radiation calculations. The prognostic cloud condensate scheme is primarily used to supply the longwave and shortwave radiative properties of clouds for CAM2 (e.g., Zhang et al. 2003) and those versions of CCM3 employing this scheme. Figure 4 shows the latitudinal distribution of CCM3 and CAM2 total cloud fraction for winter and summer over high southern latitudes. At least two very different cloud regimes exist south of 65°S, including the coastal region where the oceanic influence is large and the cold interior where the aerosol

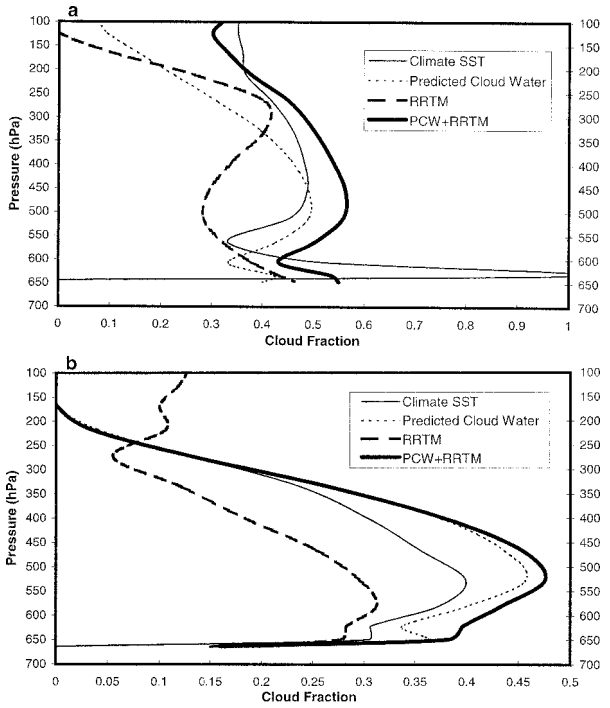

FIG. 5. Vertical profiles of 3-month average cloud fraction for (a) winter and (b) summer at the South Pole.

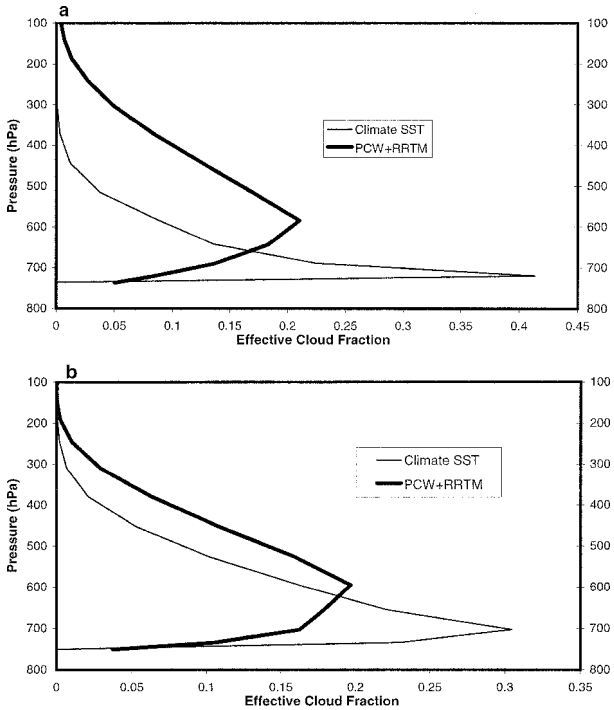

FIG. 6. Vertical profiles of 3-month average effective cloud fraction for (a) winter and (b) summer for 80°–90°S.

concentration can be very small. It would be unreasonable to presume that any simple cloud scheme can fully represent the broad range of cloud formation processes that occur across different climatic regimes. The CCM3 total cloud fraction over interior Antarctic is primarily from middle-level clouds, with low-level clouds providing the largest contribution over the Southern Ocean. The different configurations of CCM3 have similar diagnosed values of total cloud fraction. During summer, total cloud fraction is large near the latitudes of the Antarctic coastline, and decreases south of 65°S, in basic agreement with observations (Fig. 4b). The values south of 85°S appear to be somewhat larger than the observed values from Hahn et al. (1995).

During winter, diagnostic cloud fraction has much less agreement with observations (Fig. 4a). Again, middle-level clouds dominate the contribution to total cloud fraction over interior Antarctica. The total cloud fraction is about 80% near the coastal latitudes, more or less reflecting the large observed cloudiness there. The model cloud fraction, however, increases to the south unlike the observed values. Near the South Pole, total cloud fraction is about 90%, perhaps more than twice the observed fraction. The Slingo-type scheme may work especially poorly under the extreme cold conditions over the Antarctic plateau because the saturation vapor pressure with respect to ice is extremely small; thus, the atmosphere is likely to be close to saturation or even supersaturated with respect to ice. Given the frequent occurrence of clear-sky precipitation at these latitudes, visible clouds can easily be absent even when the relative humidity is high (Bromwich 1988).

Figure 5 shows the vertical distribution of cloud fraction. For the CCM3 simulations with the standard cloud parameterizations there is a sharp winter maximum in the boundary layer at the model's second lowest level ($\sigma = 0.9705$) with cloud fraction rapidly decreasing above that level. This is a consequence of the Slingo-type of cloud fraction parameterization and the cold temperatures within the Antarctic boundary layer. The winter cloud fraction profile in Fig. 5a apparently captures some of the bimodal distribution observed by Mahesh et al. (2001a) because there is also a relatively large cloud fraction between 300 and 500 hPa. The predicted cloud condensate scheme shifts the location of highest cloud fraction upward in the troposphere. During summer, the simulated cloud fraction has a maximum between 500 and 550 hPa.

While the cloud fraction provides some indication of the vertical location of clouds, it does not tell us how optically thick the clouds are. Therefore, we evaluate the diagnostic quantity known as effective cloud fraction that provides useful insight on the radiative impact of the clouds. Effective cloud fraction is determined by multiplying emissivity by cloud fraction. Figure 6 shows the vertical distribution of effective cloud fraction for the polar cap south of 80°S. The standard version of CCM3 has effective cloud fraction heavily weighted toward the boundary layer, where the cloud fraction was large in Fig. 5. This is especially true during winter.

There is some seasonal difference in the profiles; however, the overall cloud thickness does not show clearly larger values during either winter or summer. Rasch and Kristjánsson (1998) find that, globally, the prognostic cloud scheme increases the height of the center of mass of cloud particles. This is also seen in Fig. 6 because the maximum is moved to more than 100 hPa above the surface for PCW + RRTM. A significant amount of cloud condensate is located well above the maximum level with the use of the prognostic cloud scheme. Given that the maximum should occur somewhere above the cloud base, the vertical profile for CCM3 simulations with the prognostic cloud scheme is not inconsistent with the observations of Mahesh et al. (2001a,b). They also find that observed higher base clouds are thinner, which is consistent with the lower effective cloud fraction above the maximum level. Thus, CCM3's vertical profile of effective cloud fraction appears to be qualitatively realistic with the use of the prognostic cloud scheme. With the prescribed vertical distribution of cloud condensate in the standard version of CCM3, the maximum effective cloud fraction at level 17 of the 18 sigma levels results in ''cloud-top'' radiative cooling in the boundary layer. The annual average longwave contribution to temperature change at sigma level 17 is -12.3 K day^{-1} at the South Pole in the AMIP SST run. The rate is an order of magnitude smaller, -1.3 K day^{-1} in the Predicted Cloud Water simulation. The excessive longwave cooling contributes to the spurious minimum in temperature above the surface seen in Fig. 2 for the simulations without prognostic cloud condensate. On the other hand, it is less certain whether the vertical profile of effective cloud fraction in Fig. 6 is quantitatively realistic for PCW + RRTM. Figures 1 and 2 indicate that the temperature field might be impacted by excessive radiative effects of clouds with the use of the prognostic scheme.

6. Radiation

We now look at how the model parameterizations influence the radiation fields, especially at the earth's surface. Comparisons against the observed radiation are a good way of judging the vertically integrated impact of the clouds simulated by CCM3. Figure 7 shows the downward shortwave radiation and net (downward) shortwave radiation at the surface for the South Pole. Radiation observations are provided by J. King (1997, personal communication) and are nearly identical to the values of Dutton et al. (1989). The simulated shortwave radiation is closer to that observed during the months of January and February than during the spring months of October and November. During December, the observed downward shortwave radiation is 442.7 W m^{-2} at the surface (Fig. 7a). The NCAR climate models produce smaller values by 30–45 W m^{-2}. The absorbed shortwave radiation at the surface is consistent with this difference, because the observed value is 83.1 W m^{-2}

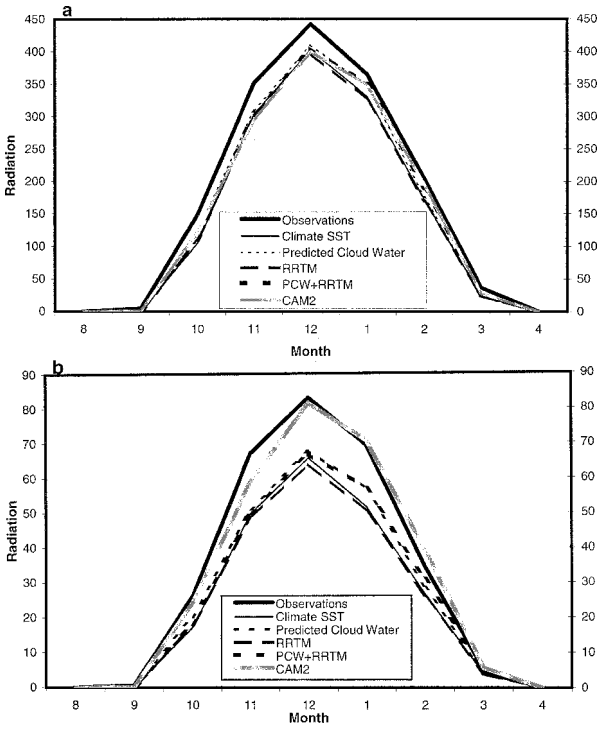

FIG. 7. Monthly surface shortwave radiation (W m^{-2}) at the South Pole for (a) the downward flux and (b) the net flux.

and the CCM3 values are 64–68 W m^{-2} during December (Fig. 7b). On the other hand, with a smaller albedo for CAM2, the absorbed shortwave is 81.5 W m^{-2}, very close to the observed value. It appears that clouds are excessively blocking shortwave radiation from reaching the surface over Antarctica. The smaller albedo in CAM2 compensates for this.

Figure 8 shows downward longwave radiation and net (upward) longwave radiation at the surface. The positive net longwave radiation implies longwave cooling at the surface. While the shortwave radiation is zero during winter, the longwave radiation is important all year long. During winter months, surface cooling by the net longwave radiation lost into the atmosphere is primarily balanced by turbulent heat flux downward from the atmosphere. Latent heat flux and the climatological heat storage rate in the ice are generally very small during winter. The surface energy balance is more complicated during summer with shortwave (longwave) radiation generally heating (cooling) the surface. Thus, there is a tendency for the longwave and shortwave radiation to balance, with latent heat flux and sensible heat flux contributions also being important. The net surface longwave radiation for the standard version of CCM3 is close to the observed value most of the year except for December when the longwave radiative cooling is too small by 10 W m^{-2}. The addition of prognostic clouds to CCM3 in other simulations, however, results in an increase in net longwave radiation. Again, the

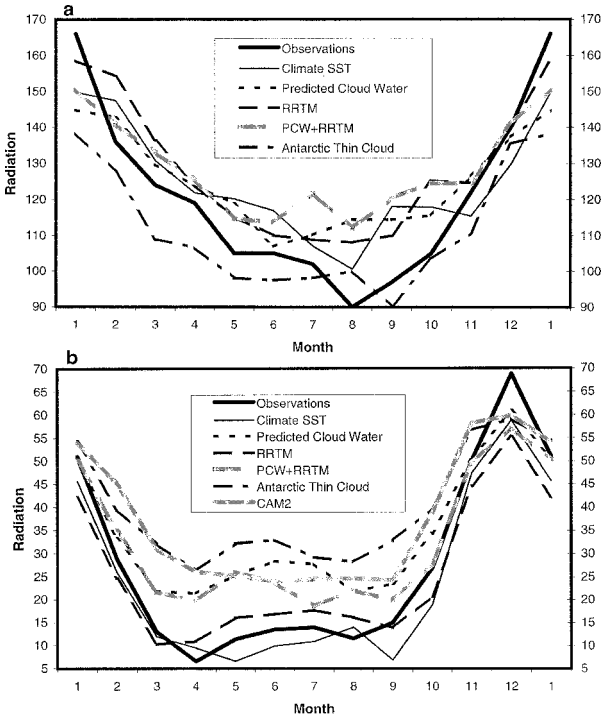

FIG. 8. Monthly surface longwave radiation (W m^{-2}) at the South Pole for (a) the downward flux and (b) the net flux.

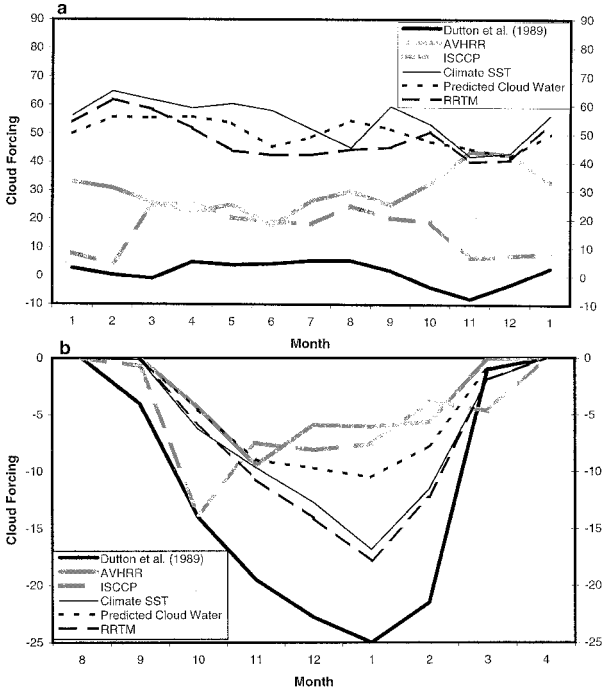

FIG. 9. Monthly surface cloud forcing (W m^{-2}) at the South Pole for (a) longwave flux and (b) shortwave flux.

change to the prognostic cloud condensate scheme has a larger impact than that of RRTM.

The downward longwave flux in the CCM3 simulations is somewhat larger than the observed value most of the year. The observed annual average is 111.6 W m^{-2}, while the simulated values are 118.6, 119.1, 121.7, and 122.2 for the Climate SST, Predicted Cloud Water, RRTM, and PCW + RRTM simulations, respectively, at the South Pole. The excess over the observed value is somewhat larger during winter, and the difference is smaller or even of the opposite sign during summer. All of these findings are consistent with significant cloud effects on the simulations. This is especially evident during winter in the absence of shortwave radiation. During summer, the cloud effects are more complicated because clouds can have a cooling effect by reflecting shortwave radiation and a warming effect by absorbing and emitting longwave radiation.

The radiative effect of clouds can be examined with cloud forcing terms. If clear-sky flux terms are available, the shortwave cloud forcing is the net (downward) shortwave flux minus the net clear-sky shortwave flux. The longwave cloud forcing is the net (upward) clear-sky longwave flux minus the net longwave flux. A positive cloud forcing indicates a warming effect of clouds. Unfortunately, not all of the CCM3 simulations have reliable clear-sky longwave flux output, which is required to calculate the cloud forcing. Reasonable estimates of clear-sky cloud forcing at the South Pole surface are available for Climate SST, Predicted Cloud Water, and RRTM. These are shown in Fig. 9. Also shown are estimates of the cloud forcing at the surface from Dutton et al. (1989) and recently derived values from satellite observations using those of the 1982–99 AVHRR and 1985–93 ISCCP (Pavolonis and Key 2003). The estimates of observed longwave cloud forcing vary considerably in Fig. 9a. The values from Dutton et al. (1989) have small magnitude, never exceeding 8 W m^{-2} in any month. Despite the variations in the different estimates of longwave cloud forcing at the South Pole surface, the CCM3 values appear to be much too large almost all year long, with an excess of 20 W m^{-2} or more. Some difference between the CCM3 values may result from different algorithms to estimate clear-sky flux. From Fig. 9a we cannot detect an increase in longwave cloud forcing resulting from the prognostic cloud condensate scheme, because the values for the Predicted Cloud Water are usually smaller than the corresponding values for Climate SST. On the other hand, the longwave cloud forcing at the top of the atmosphere (not shown) is about 7 W m^{-2} larger during summer and about 20 W m^{-2} larger during winter for Predicted Cloud Water. Thus, the prognostic cloud condensate scheme may increase the longwave radiative impact of clouds in a vertical column over Antarctica.

The shortwave cloud forcing at the surface is smaller than the longwave cloud forcing. This is not surprising given that downward longwave flux from clouds is almost entirely absorbed at the surface (emissivity is 0.97 for CCM3), while over 80% of the incident shortwave flux is reflected. The shortwave cloud forcing in Fig.

9b for CCM3 has about half of the cooling effect at the surface than the estimates of Dutton et al. (1989). On the other hand, the CCM3 values are about twice as large during summer than the values derived from AVHRR and ISCCP. The latter estimates appear to be more reliable than the earlier estimates of Dutton et al. because Fig. 7b shows that CCM3 underestimates the incident shortwave flux at the South Pole. This would imply too much reflection by clouds and an excessive shortwave cloud forcing for CCM3, consistent with values larger than those for AVHRR and ISCCP in Fig. 9b. Thus, the results shown in Fig. 9, together with excessive winter surface temperatures (Fig. 1) and insufficient incident shortwave radiation at the surface (Fig. 7b), indicate excessive longwave and shortwave radiative impacts of the Antarctic clouds. Briegleb and Bromwich (1998b) note that the cloud water path for CCM3 was excessive by perhaps a factor of 2 in the polar regions, consistent with the results shown here.

7. CCM3 simulations with increased and decreased cloud thickness

Recognizing that there were deficiencies in the CCM3 treatment of polar clouds, NCAR researchers modified the treatment of water clouds over sea ice during the development of CAM2. By altering the clouds, and, hence, the radiation at the atmosphere–sea ice interface, they were able to alleviate biases in the growth of sea ice in coupled atmosphere–sea ice simulations. The correction involved reducing the specified number density of cloud water drops in the detailed scheme that calculates the autoconversion of suspended in-cloud liquid water to rainwater that falls toward the earth's surface. In the climate model simulations, autoconversion is a key sink to atmospheric moisture substance. Furthermore, a diagnosed radius of liquid drops is inversely proportional to the specified number density (Rasch and Kristjánsson 1998). Hence, the reduced density increases the size of water drops. Precipitation now occurs more readily in the parameterized scheme because the increased drop radii more easily exceed a critical value for the onset of precipitation (Rasch and Kristjánsson 1998). In CAM2, the number density over sea ice was set at 5 cm^{-3} instead of the CCM3 oceanic value of 150 cm^{-3}. Therefore, rain occurs more readily over sea ice in CAM2. This alteration, however, only impacts liquid precipitation. The parameterization for autoconversion of cloud ice to snow is simpler and does not involve a specified particle number density. Because clouds over the Antarctic continent are largely composed of ice crystals, the modified autoconversion of liquid cloud condensate to precipitation has little impact over Antarctica. A test performed by the authors has verified this.

In contrast to that of liquid water precipitation, CCM3's prognostic parameterization for autoconversion from suspended ice cloud to snow follows Kessler (1969) and is parameterized by a simple expression,

$$\text{Autoconversion} = C(q_{\text{ice}} - q_{\text{threshold}}), \qquad (1)$$

where C is a constant. The cloud ice mixing ratio q_{ice} must exceed a specified threshold $q_{\text{threshold}}$ for autoconversion to take place. The threshold is temperature sensitive and set at 5×10^{-6} for temperatures below -20°C, which are commonly found over interior Antarctica, even for the summer boundary layer.

There are few observations of ice cloud mass content over Antarctica that can be compared against the specifications for the autoconversion parameterization. Stone (1993) derived the ice content of clouds at the South Pole from radiation measurements. He expresses cloud thickness in terms of density. His values range from 0.3×10^{-6} to 6.0×10^{-6} kg m^{-3}. The CCM3 threshold is given in units of mixing ratio (ice cloud mass per air mass). The lower-tropospheric air density over the high Antarctic plateau is typically in the range of 0.75–1.0 kg m^{-3}. Therefore, the threshold cloud mass density for ice precipitation (5×10^{-6} times air density) would be from 3.75×10^{-6} to 5.0×10^{-6} kg m^{-3}. This range is toward the higher end of Stone's observed thickness, so the ice clouds must be relatively thick by Antarctic standards for autoconversion in CCM3. The model CAM2 also uses the same ice autoconversion parameterization. On the other hand, the presence of ''clear-sky'' precipitation (Miller 1974; Smiley et al. 1980) without visible clouds suggests that a low threshold is required for the initiation of precipitation over Antarctica. Thus, it is natural that we investigate the impact of a modified threshold for ice autoconversion.

To test the sensitivity of Antarctic clouds to the threshold, a simulation referred to as Thin Cloud is performed with the cloud ice mixing ratio for autoconversion set at 1.0×10^{-6} instead of 5×10^{-6}. This new threshold value is representative of the middle of Stone's (1993) observed range. The new simulation is carried out for 15 yr with the same boundary conditions as PCW + RRTM. Furthermore, a 5-yr simulation referred to as Thick Cloud is performed with the threshold set at the increased value 10×10^{-6}. Both of the new simulations have the RRTM longwave radiation scheme and prognostic clouds. Thus, they are directly comparable to PCW + RRTM.

The vertical distributions of effective cloud fraction for the new simulations are shown in Fig. 10. During winter, the effective cloud fraction is approximately twice as large in Thick Cloud than in Thin Cloud. The maximum value remains at the same level. During summer, there is only a slight change in cloud thickness in the boundary layer due to the threshold change. The effective cloud fraction, however, is significantly reduced in Thin Cloud above 600 hPa. Because the cloud fractions (not shown) are similar for the simulations, the emissitivity differs by about a factor of 2 during winter, and somewhat less than that at most tropospheric

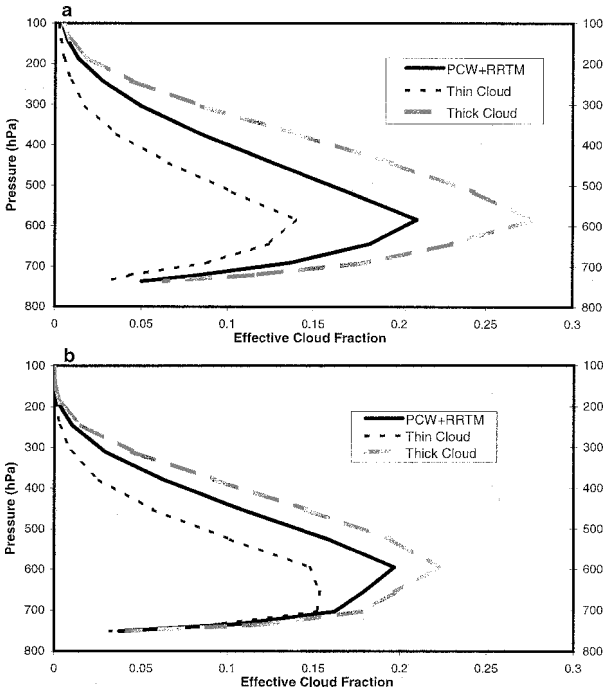

FIG. 10. Vertical profiles of 3-month average effective cloud fraction during (a) winter and (b) summer for the PCW + RRTM, Thick Cloud, and Thin Cloud simulations for 80°–90°S.

levels during summer. Therefore, the simulations should be sensitive to the parameters of the simple ice autoconversion parameterization. The Thin Cloud experiment may provide for an improved simulation of the Antarctic climate, because it has thinned radiative clouds compared to the apparently thick clouds in other CCM3 simulations.

The results of the Thin Cloud experiment are included in Figs. 8, 11, and 12. During winter, the surface temperature at the South Pole is about 5°C colder in the experiment with the reduced ice autoconversion threshold than for the simulation PCW + RRTM (Fig. 11). The difference is largely confined to the boundary layer (Fig. 12). Because the emissivity of the clouds is reduced, the downward longwave radiation for Thin Cloud is reduced by 10–20 W m^{-2} from the values for PCW + RRTM (Fig. 8a). Interestingly, the downward longwave flux for Thin Cloud is actually smaller than that observed at the surface for all months except August. The small downward longwave flux is probably a consequence of the CCM3 tendency toward cold tropospheres above the boundary layer (Figs. 2 and 12). While the reduced surface temperatures in Thin Cloud bring the upward longwave radiation closer to observations (not shown), the net longwave radiation field is not necessarily improved by the reduced autoconversion threshold. Figure 8b shows that the net surface radiation is larger than the observed value by as much as 20 W m^{-2} during winter for this experiment. This excess over that observed is roughly double the excess

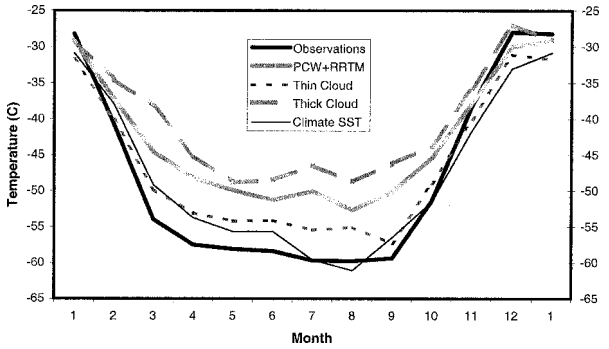

FIG. 11. Monthly surface temperature (°C) at the South Pole.

for PCW + RRTM. The excess is manifested in increased emitted radiation from the warmer-than-observed surface during winter and insufficient downward radiation, especially during summer when the cold bias is most pronounced (Fig. 12b).

The bias in net longwave radiation is balanced during winter by heat flux downward from the atmosphere. Sensible heat flux for the South Pole is shown in Fig. 13a. The thick solid line shows observations from the Patrick Automatic Weather Station at 89.88°S for the year 1986 (Stearns and Weidner 1993). Climatological observations from the South Pole supplied by J. King (1997, personal communication) indicate a winter value of about −10 W m^{-2}, more or less in agreement with

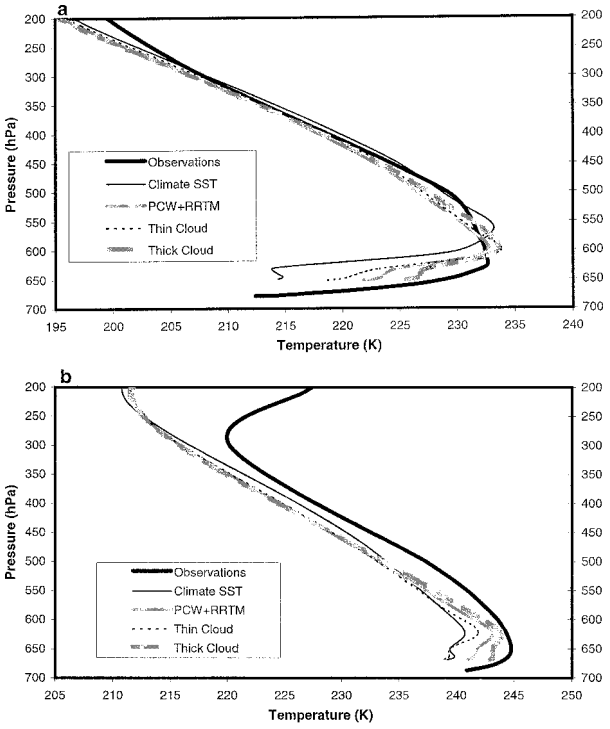

FIG. 12. Vertical profiles of 3-month average temperature (K) from observations and model results at the South Pole for (a) winter and (b) summer.

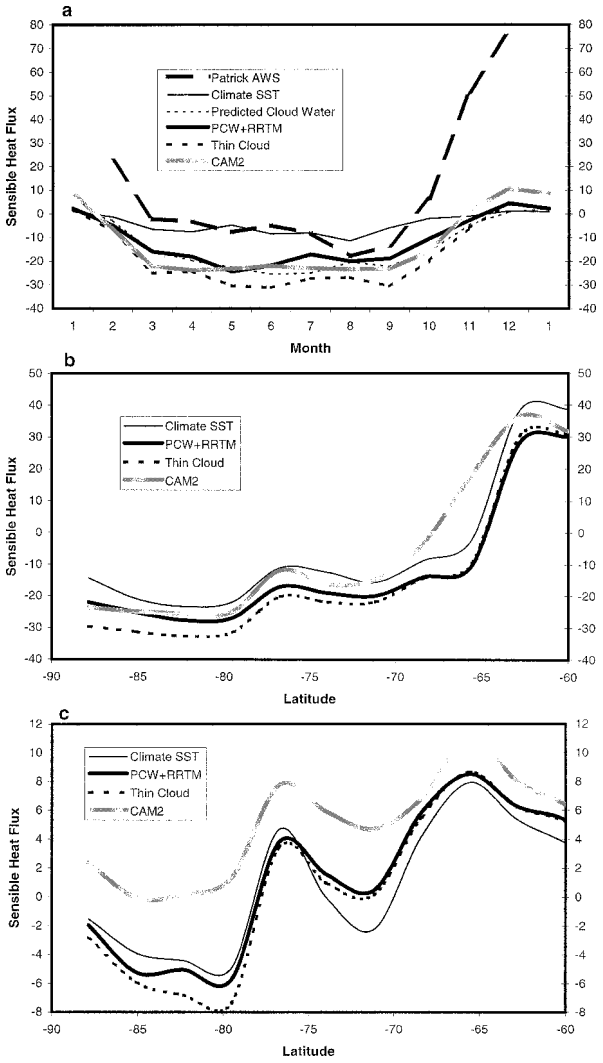

FIG. 13. Sensible heat flux (W m^{-2}) displayed as (a) monthly values at the South Pole, (b) 3-month average for winter, and (c) 3-month average for summer as a function of latitude.

1986 values for Patrick. The summer values for Patrick appear to be excessive, because the climatological values from King indicate a combined sensible and latent heat flux of about 10 W m^{-2}. Figures 8b and 13a show that during winter there is an approximate balance between sensible heat flux and the net longwave radiation at the surface. During both summer and winter the sensible heat flux is negative (heat is transported downward from the atmosphere to the ice surface) over interior Antarctica for the NCAR models (Figs. 13b and 13c). The exception is the summer sensible heat flux for CAM2, which is slightly positive at some latitudes south of 80°S. Apparently, the warm bias connected with the lower surface albedo for CAM2 sometimes results in heat flux from the surface to the atmospheric boundary layer. Figure 13 also shows that the CCM3 heat flux from the atmosphere to the surface is larger for Thin Cloud than other simulations. This is particularly true for winter when the zonal average magnitude can exceed 30 W m^{-2}. The net longwave radiation has similar magnitude for the Thin Cloud experiment (Fig. 8b).

Thus, while the reduced autoconversion threshold for CCM3 ice clouds has reduced the longwave cloud emissitivity, which should be an improvement to the simulation, it has also exacerbated an improper surface energy balance in simulations with prognostic cloud water. This improper balance exists for the CCM3 Predicted Cloud Water and Thin Cloud simulations, as well as for CAM2, which also has the prognostic cloud scheme (Fig. 8b). The observed surface net longwave radiation is generally small, with a magnitude less than 15 W m^{-2} at the South Pole during winter. This is largely balanced by the sensible heat flux of a similar magnitude, because the heat storage is generally small over climatological time scales. The small heat flux occurs in spite of the generally large vertical temperature gradient in the Antarctic boundary layer. The average magnitude of the observed inversion strength is about 20°C for the South Pole winter. Very high static stability suppresses heat transfer between the ice surface and the atmosphere. The detailed structure of the inversion, however, is often not well captured by numerical models with coarse vertical resolution of the shallow Antarctic boundary layer. King (1990) finds that the surface similarity theory may not hold at heights above 5–10 m for the very stable boundary layer at Halley, Antarctica. Moreover, Cassano et al. (2001) note that if a model's vertical resolution is too coarse to represent the very stable surface layer then the downward sensible heat flux will probably be overestimated. The CCM3 has a lowest level typically 50 m above the Antarctic plateau surface. Consequently, excessive heat flux can be expected. For the standard version of CCM3, however, the sensible heat flux is somewhat suppressed by spurious temperature minima above the surface in the lower boundary layer, as seen in Fig. 2a. With the inclusion of the prognostic cloud scheme, the temperature profiles in Fig. 2 are altered, more accurately reflecting the strong inverted lapse rate within the inversion. The smoother temperature profile, however, allows the increased heat flux seen in Fig. 13. An additional effect of CCM3's tendency to overestimate the magnitude of the sensible heat flux may be a delay in the onset of very cold surface temperature as winter approaches. Notice that the observed surface temperature is colder than that simulated during March and April in Fig. 1a, while Fig. 13a indicates that the simulated magnitude of the surface heating by turbulent flux is too large during these months. Because few current global climate models adequately resolve the very shallow surface boundary layer, attention must be paid to the boundary layer problem to achieve an improved simulation of the Antarctic surface energy balance. Future efforts at modeling Antarctic clouds and radiation should address both the cloud radiative properties and the boundary layer.

8. Summary and conclusions

Simulations with the NCAR CCM3 and the newest generation NCAR climate model CAM2 are evaluated for their treatment of clouds and radiation over Antarctica. The present study expands upon the earlier work of Briegleb and Bromwich (1998a,b), which detailed the radiation budget and polar climate of CCM3. Our knowledge of the success of parameterizations within global climate models for high southern latitudes has been limited previously, due to both sparse observational work on the radiative properties of Antarctic clouds and emphasis on developing parameterizations relevant for other climates.

To study and consider improvements upon the parameterizations of clouds and radiation, the Rasch and Kristjánsson (1998) prognostic cloud condensate scheme and the RRTM longwave radiative transfer algorithm have been included in a version of CCM3. The Rasch and Kristjánsson scheme obtains cloud optical properties from the simulated cloud condensate, whereas the standard scheme obtains optical properties from diagnostic clouds. The RRTM alleviates the deficit in downward clear-sky longwave radiation (Mlawer et al. 1997; Briegleb and Bromwich 1998b). The Rasch and Kristjánsson scheme is now the standard cloud scheme for CAM2. The RRTM is not included in CAM2. Nevertheless, the new longwave radiation parameterization for CAM2 has similar properties to RRTM because it alleviates the clear-sky bias and produces good agreement with line-by-line radiation calculations (Collins et al. 2002). Simulations with a standard version of CCM3 are compared to those with RRTM and the standard diagnostic clouds, the standard longwave scheme and the prognostic cloud scheme, and both RRTM and prognostic clouds. The simulations show a cold bias in the troposphere above the Antarctic boundary layer, especially during summer. The cold bias is as large as 20 K for the summer stratosphere.

The changes resulting from the introduction of prognostic clouds are much larger than those resulting from the introduction of RRTM. The prognostic cloud scheme results in increased cloud emissivity in the upper troposphere, reduced cloud emissivity in the lower troposphere, and a qualitatively improved vertical distribution of cloud radiative properties over interior Antarctica, compared to simulations with standard diagnostic clouds. Significant deficiencies are found in the simulation of Antarctic cloud radiative effects. The optical thickness of Antarctic clouds appears to be excessive, consistent with the findings of Briegleb and Bromwich (1998b). This results in a warm bias in surface temperature during winter and a deficit in downward shortwave radiation at the surface during summer. Several biases in the CCM3 simulations are larger with the prognostic cloud condensate scheme than with the standard diagnostic cloud scheme. The representations of Antarctic clouds and radiation by early versions of the new NCAR CAM2 are not clearly improved compared to those of the earlier CCM3. For example, the surface albedo over Antarctica is decreased in CAM2 and CCSM2 simulations in comparison to CCM3 simulations. This change contributes to a warm bias in tropospheric temperature during summer.

To test the sensitivity of CCM3 to the mixing ratio threshold for autoconversion from suspended ice cloud to falling precipitation, the threshold is given increased or decreased values in sensitivity simulations. The emissivity of Antarctic clouds is found to be highly sensitive to the threshold, especially during winter. When the threshold is reduced toward a more realistic value, the Antarctic clouds are thinned and some of the biases in the temperature and radiation fields are reduced. However, the vertical resolution of the very shallow, very stable boundary layer is apparently insufficient to properly calculate the sensible heat flux. This leads to an improper winter balance between sensible heat flux and net longwave radiation at the surface. Both fields have excessive values. To improve the simulation of the surface energy balance, not only must the radiative effects of clouds be improved, it is also necessary to improve the boundary layer treatment.

Researchers at NCAR are aware of biases for the Tropics, midlatitudes, and polar regions in early versions of CAM2. In response to these concerns, considerable efforts have gone into a revised version of CAM2, which is expected to be released to the public in the near future. A fall speed for cloud particles was introduced. This should help to thin the polar clouds. Initial reports are said to be encouraging regarding the efforts to alleviate biases in the polar regions and elsewhere. Future efforts at improving cloud parameterizations for the polar regions should be based upon this new version. The studies on Antarctic clouds presented here have helped to encourage recent model development. Future work should also consider clear-sky precipitation and the radiative effects of nonspherical cloud ice particles. Renewed field studies are also needed to provide a better database on Antarctic clouds to facilitate comparisons between model parameterizations and observations.

Acknowledgments. This project is supported by National Science Foundation via Grant NSF-ATM-9820042 and by NASA via Grant NAG5-7750. The CCM3 simulations were performed with Project 36091005 at NCAR, which is supported by NSF and Grant PAS0689 from the Ohio Supercomputer Center, which is supported by the State of Ohio. The AVHRR and ISCCP data are obtained from the Cooperative Institute for Meteorological Satellite Studies at the University of Wisconsin—Madison. The automatic weather station data are obtained from the Antarctic Meteorological Research Center. James Rosinski of NCAR provided output from standard configuration simulations of the NCAR climate models. Graduate students Chris Hennon and Rahul George have helped run the CCM3

simulations. We thank Dan Lubin, Von Walden, Austin Hogan, and Tom DeFelice for their helpful advice.

REFERENCES

Anderson, P. S., 1993: Evidence for an Antarctic winter coastal polynya. *Antarct. Sci.,* **5,** 221–226.

Bonan, G. B., 1996: A land surface model (LSM version 1.0) for ecological, hydrological, and atmospheric studies: Technical description and user's guide. NCAR Tech. Note, NCAR/TN-417+STR, 150 pp.

Briegleb, B. P., and D. H. Bromwich, 1998a: Polar climate simulation of the NCAR CCM3. *J. Climate,* **11,** 1270–1286.

——, and ——, 1998b: Polar radiation budgets of the NCAR CCM3. *J. Climate,* **11,** 1246–1269.

Bromwich, D. H., 1988: Snowfall in high southern latitudes. *Rev. Geophys.,* **26,** 149–168.

Cassano, J. J., T. R. Parish, and J. C. King, 2001: Evaluation of turbulent flux parameterizations for the stable surface layer over Halley, Antarctica. *Mon. Wea. Rev.,* **129,** 26–46.

Collins, W. D., 2001: Parameterization of generalized cloud overlap for radiative calculations in general circulation models. *J. Atmos. Sci.,* **58,** 3224–3242.

——, J. K. Hackney, and D. P. Edwards, 2002: An updated parameterization for infrared emission and absorption by water vapor in the National Center for Atmospheric Research Community Atmosphere Model. *J. Geophys. Res.,* **107,** 4664, doi:10.1029/2001JD001365.

——, and Coauthors, 2003: Description of the NCAR Community Atmosphere Model (CAM2). NCAR Tech. Note, in press. [Available online at http://www.ccsm.ucar.edu/models/atm-cam/docs/description/index.html.]

Curry, J. A., W. B. Rossow, D. Randall, and J. L. Schramm, 1996: Overview of Arctic cloud and radiation characteristics. *J. Climate,* **9,** 1731–1764.

——, and Coauthors, 2000: FIRE Arctic clouds experiment. *Bull. Amer. Meteor. Soc.,* **81,** 5–29.

Dutton, E. G., R. S. Stone, and J. L. Deluisi, 1989: South Pole surface radiation balance measurements April 1986 to February 1988. NOAA Data Rep. ERL ARL-17, 49 pp.

Ebert, E. E., and J. A. Curry, 1992: A parameterization of ice cloud optical properties for climate models. *J. Geophys. Res.,* **97,** 3831–3836.

Gates, W. L., and Coauthors, 1996: Climate models—Evaluation. *Climate Change 1996,* J. T. Houghton et al., Eds., Cambridge University Press, 233–284.

Girard, E., and J. A. Curry, 2001: Simulation of Arctic low-level clouds observed during the FIRE Arctic clouds experiment using a new bulk microphysics scheme. *J. Geophys. Res.,* **106,** 15 139–15 154.

Hack, J. J., B. A. Boville, B. P. Briegleb, J. T. Kiehl, P. J. Rasch, and D. L. Williamson, 1993: Description of the NCAR Community Climate Model (CCM2). NCAR Tech. Note, NCAR/TN-382+STR, 108 pp.

Hahn, C., S. Warren, and J. London, 1995: Climatological data for clouds over the globe from surface observations, 1982–1991: Data tape documentation for the total cloud edition. Carbon Dioxide Information Analysis Center Numerical Data Package NDP-026A, 39 pp. [Available from Carbon Dioxide Information Analysis Center, Oak Ridge National Laboratory, Oak Ridge, TN 37831.]

Iacono, M. J., E. J. Mlawer, S. A. Clough, and J.-J. Morcrette, 2000: Impact of an improved longwave radiation model, RRTM, on the energy budget and thermodynamic properties of the NCAR Community Climate Model, CCM3. *J. Geophys. Res.,* **105,** 14 873–14 890.

Kessler, E., 1969: *On the Distribution and Continuity of Water Substance in Atmospheric Circulations. Meteor. Monogr.,* No. 32, Amer. Meteor. Soc., 84 pp.

Key, J., 2001: The Cloud and Surface Parameter Retrieval (CASPR) system for polar AVHRR data user's guide. Space Science and Engineering Center, University of Wisconsin—Madison, 62 pp.

Kiehl, J. T., J. J. Hack, G. B. Bonan, B. A. Boville, D. L. Williamson, and P. J. Rasch, 1998a: The National Center for Atmospheric Research Community Climate Model: CCM3. *J. Climate,* **11,** 1131–1149.

——, ——, and J. W. Hurrell, 1998b: The energy budget of the NCAR Community Climate Model: CCM3. *J. Climate,* **11,** 1151–1178.

King, J. C., 1990: Some measurements of turbulence over an Antarctic ice shelf. *Quart. J. Roy. Meteor. Soc.,* **116,** 379–400.

Kristjánsson, J. E., J. M. Edwards, and D. L. Mitchell, 1999: A new parameterization scheme for the optical properties of ice crystals for use in general circulation models of the atmosphere. *Phys. Chem. Earth,* **24,** 231–236.

Lubin, D., and D. A. Harper, 1996: Cloud radiative properties over the South Pole from AVHRR infrared data. *J. Climate,* **9,** 3405–3418.

——, B. Chen, D. H. Bromwich, R. C. J. Somerville, W.-H. Lee, and K. M. Hines, 1998: The impact of Antarctic cloud radiative properties on a GCM climate simulation. *J. Climate,* **11,** 447–462.

Mahesh, A., V. P. Walden, and S. G. Warren, 1997: Radiosonde temperature measurements in strong inversions: Correction for thermal lag based on an experiment at the South Pole. *J. Atmos. Oceanic Technol.,* **14,** 45–53.

——, ——, and ——, 2001a: Ground-based infrared remote sensing of cloud properties over the Antarctic Plateau. Part I: Cloud-base heights. *J. Appl. Meteor.,* **40,** 1265–1278.

——, ——, and ——, 2001b: Ground-based infrared remote sensing of cloud properties over the Antarctic Plateau. Part II: Cloud optical depths and particle sizes. *J. Appl. Meteor.,* **40,** 1279–1294.

Marshall, S. E., 1989: A physical parameterization of snow albedo for use in climate models. NCAR Cooperative thesis NCAR/CT-123, 161 pp.

Miller, S. A., 1974: Inversion layer over the Antarctic Plateau, for steady state conditions. Ph.D. dissertation, University of Wisconsin—Madison, 68 pp.

Mlawer, E. J., S. J. Taubman, P. D. Brown, M. J. Iacono, and S. A. Clough, 1997: Radiative transfer for inhomogeneous atmospheres: RRTM, a validated correlated-k model for the longwave. *J. Geophys. Res.,* **102,** 16 663–16 682.

Morely, B. M., E. E. Uthe, and W. Viezee, 1989: Airborne lidar observations of clouds in the Antarctic troposphere. *Geophys. Res. Lett.,* **16,** 491–494.

Pavolonis, M. J., and J. Key, 2003: Antarctic cloud radiative forcing at the surface estimated from the AVHRR Polar Pathfinder and ISCCP D1 datasets, 1985–93. *J. Appl. Meteor.,* **42,** 827–840.

Pinto, J. O., and J. A. Curry, 1997: Role of radiative transfer in the modeled mesoscale development of summertime Arctic stratus. *J. Geophys. Res.,* **102,** 13 861–13 872.

——, ——, and A. H. Lynch, 1999: Modeling clouds and radiation for the November 1997 period of SHEBA using a column climate model. *J. Geophys. Res.,* **104,** 6661–6678.

Randall, D., and Coauthors, 1998: Status of and outlook for large-scale modeling of atmosphere–ice–ocean interactions in the Arctic. *Bull. Amer. Meteor. Soc.,* **79,** 197–219.

Rasch, P. J., and J. E. Kristjánsson, 1998: A comparison of the CCM3 model climate using diagnosed and predicted condensate parameterizations. *J. Climate,* **11,** 1587–1614.

Schwerdtfeger, W., 1984: *Weather and Climate of the Antarctic.* Elsevier, 261 pp.

Shibata, K., and M. Chiba, 1990: Effects of radiation scheme on the surface and wind regime over the Antarctic and on circumpolar lows. *NIPR Symp. Polar Meteor. Glaciol.,* **3,** 58–78.

Slingo, A., 1989: GCM parameterization for the shortwave radiative properties of water clouds. *J. Atmos. Sci.,* **46,** 1419–1427.

Slingo, J. M., 1987: The development and verification of a cloud

prediction scheme for the ECMWF model. *Quart. J. Roy. Meteor. Soc.*, **113,** 899–927.

Smiley, V. N., B. M. Whitcomb, B. M. Morley, and J. A. Warburton, 1980: Lidar determinations of atmospheric ice crystal layers at South Pole during clear-sky precipitation. *J. Appl. Meteor.*, **19,** 1074–1090.

Stearns, C. R., and G. A. Weidner, 1993: Sensible and latent heat flux estimates in Antarctica. *Antarctic Meteorology and Climatology: Studies Based on Automatic Weather Stations*, D. H. Bromwich and C. R. Stearns, Eds., Antarctic Research Series, Vol. 61, Amer. Geophys. Union, 109–138.

Stone, R. R., 1993: Properties of Austral winter clouds derived from radiometric profiles at the South Pole. *J. Geophys. Res.*, **98,** 12 961–12 971.

Tzeng, R.-Y., D. H. Bromwich, and T. R. Parish, 1993: Present-day Antarctic climatology of the NCAR Community Climate Model version 1. *J. Climate*, **6,** 205–226.

——, ——, ——, and B. Chen, 1994: NCAR CCM2 simulation of the modern Antarctic climate. *J. Geophys. Res.*, **99,** 23 131–23 148.

Zhang, M., W. Lin, C. S. Bretherton, J. J. Hack, and P. J. Rasch, 2003: A modified formulation of fractional stratiform condensation rate in the NCAR Community Atmospheric Model (CAM2). *J. Geophys. Res.*, **108,** 4035, doi:10.1029/2002JD002523.